

SUPPORTING INFORMATION

Electronic Couplings and Rates of Excited State Charge Transfer Processes at the Poly(thiophene-co-quinoxaline)–PC₇₁BM Interfaces: Two- versus Multi-state Treatments

Tuuva Kastinen,^{*a} Demetrio Antonio da Silva Filho,^b Lassi Paunonen,^c Mathieu Linares,^d Luiz Antonio Ribeiro Junior,^b Oana Cramariuc,^e and Terttu I. Hukka^{*a}

^a Chemistry and Advanced Materials, Faculty of Engineering and Natural Sciences, Tampere University, P.O. Box 541, FI-33014 Tampere University, Finland. E-mail: tuuva.kastinen@tuni.fi, terttu.hukka@tuni.fi

^b Institute of Physics, University of Brasília, Brasília, DF, Brazil.

^c Mathematics, Faculty of Information Technology and Communication Sciences, Tampere University, P.O. Box 692, FI-33014 Tampere University, Finland.

^d Department of Physics, Chemistry and Biology (IFM), Linköping University, Linköping, Sweden.

^e Physics, Faculty of Engineering and Natural Sciences, Tampere University, P.O. Box 692, FI-33014 Tampere University, Finland; Centrul IT pentru Stiinta si Tehnologie, Av. Radu Beller 25, Bucharest, Romania.

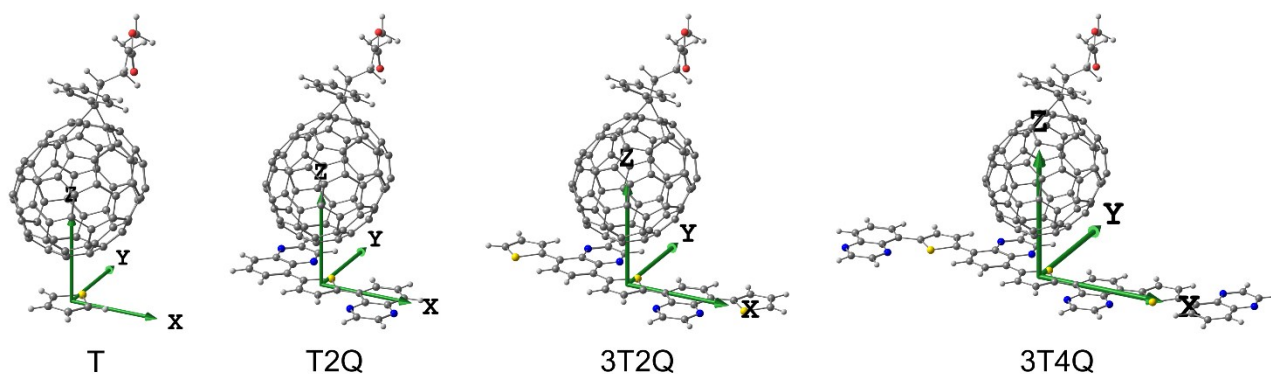
Contents

Models: studied TQ–PC ₇₁ BM complexes	S2
Methods: additional details	S3–S8
Results: additional details	
Excited state characteristics of the isolated TQ and PC ₇₁ BM models and TQ–PC ₇₁ BM complexes	S8–S10
Optimally tuned range separation parameters of the selected isolated TQ and PC ₇₁ BM models and TQ–PC ₇₁ BM complexes	S11
Excitation energies of the 3T4Q–PC ₇₁ BM and 3Q4T–PC ₇₁ BM complexes	S11–S13
Adiabatic and diabatic dipole moments and charge differences of the CT ₁ and LE states	S14–S15
NTOs of the 3T4Q–PC ₇₁ BM complex	S16
Electronic couplings of 3T4Q–PC ₇₁ BM and 3Q4T–PC ₇₁ BM	S17–S21
Bond length alternations of 3T4Q and 3Q4T	S22

Models: studied TQ-PC₇₁BM complexes

The lengths of the TQ oligomers were increased symmetrically by adding either thiophene (T) or quinoxaline (Q) units to the chain ends (Figure S1). In the first series, referred to as the T-series hereafter, the T unit was in the middle of the sequences T, QTQ (T2Q), TQTQT (3T2Q), and QTQTQTQ (3T4Q), whereas in the second series, referred to as the Q-series hereafter, the Q unit was in the middle unit of the sequences Q, TQT (Q2T), QTQTQ (3Q2T), and TQTQTQT (3Q4T). Hereafter, the TQ oligomers will be referred to with the abbreviations given in parentheses. In the TQ-PC₇₁BM complexes (Figure S1 and Figure 2 in the main article), TQ was oriented along the x-axis in the xy-plane and PC₇₁BM was placed above TQ along the z-axis. In the T-series, PC₇₁BM was placed on top of the middle thiophene (the D unit) of each oligomer by superposing the centroid of the bottom benzene ring of PC₇₁BM with the centroid of thiophene (Figure 2a in the main article). Similarly, in the Q-series, PC₇₁BM was placed above the middle quinoxaline (the A unit) by superposing the centroid of the benzene ring of PC₇₁BM with the centroid of the benzene ring in quinoxaline.

T-series



Q-series

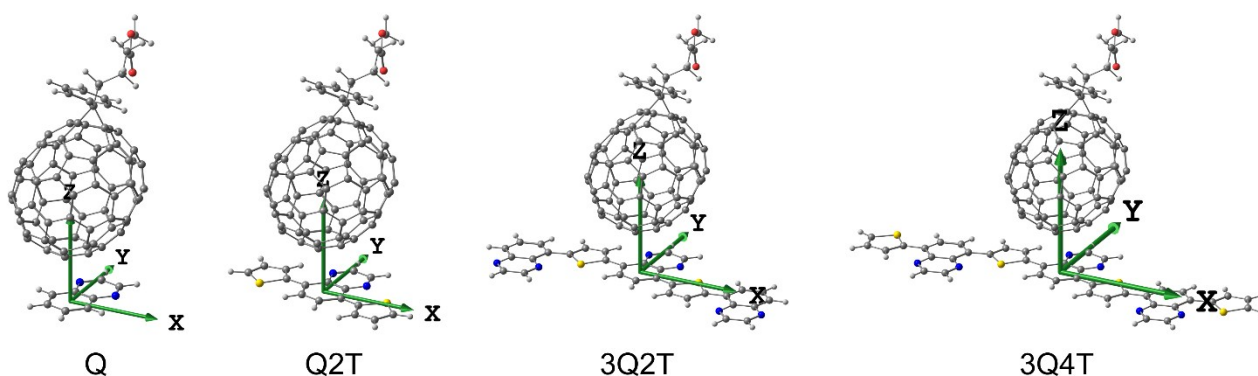


Figure S1 Studied TQ-PC₇₁BM complexes with PC₇₁BM either above thiophene (T-series) or quinoxaline (Q-series) of TQ.

Methods: additional details

The tuning of the range-separation parameter. The tuning of the range-separation parameter (ω) of the Baer–Neuhauser–Livshits (BNL)^{1,2} (originally 0.5 bohr⁻¹) LRC functional for the studied TQ–PC₇₁BM complexes was carried out with the modified version of the ionization energy (IE) tuning procedure^{3–6} in the same manner as in our previous study⁷:

$$J(\omega) = \left| \varepsilon_{\text{HOMO}}^{\omega}(N) + E_{\text{TQ}}^{\omega}(N-1) - E_{\text{TQ}}^{\omega}(N) \right| + \left| \varepsilon_{\text{HOMO}}^{\omega}(M+1) + E_{\text{PC}_{71}\text{BM}}^{\omega}(M) - E_{\text{PC}_{71}\text{BM}}^{\omega}(M+1) \right| \quad (\text{S1})$$

where $\varepsilon_{\text{HOMO}}(N)$ and $\varepsilon_{\text{HOMO}}(M+1)$ are the HOMO energies for the neutral TQ and the anion of PC₇₁BM, respectively, $E_{\text{TQ}}^{\omega}(N)$ and $E_{\text{PC}_{71}\text{BM}}^{\omega}(M)$ are the total energies of the neutral TQ and PC₇₁BM, respectively, and $E_{\text{TQ}}^{\omega}(N-1)$ and $E_{\text{PC}_{71}\text{BM}}^{\omega}(M+1)$ are the total energies of the cation of TQ and the anion of PC₇₁BM, respectively. We also checked the optimally tuned (OT) ω for the isolated TQ and PC₇₁BM molecules with the gap tuning procedure^{8,9}. In the tuning of ω , all the calculations were carried out as the SP calculations at the B3LYP/6-31G** -optimized neutral GS geometries of TQ and PC₇₁BM to keep the geometries consistent in the electronic coupling and CT rate calculations. The optimal OT ω for the isolated TQ oligomers, PC₇₁BM, and the selected TQ–PC₇₁BM complexes (3T4Q–PC₇₁BM and 3Q4T–PC₇₁BM) are given in Table S1.

Assignment of the states. Among the calculated adiabatic and diabatic states of the TQ–PC₇₁BM complexes, we have considered the GS [eD–eA], the LE state of TQ [eD*–eA], and the lowest CT state [CT₁, eD⁺–eA⁻], as they are the relevant states for the ED and CR processes (Figure 1 in the main article). In the 2- and 3-state GMH and FCD schemes, the adiabatic LE and CT₁ states were manually identified and selected on the basis of their electric dipole moments relative to the GS ($\Delta\mu_{\text{ii}}$ in the adiabatic dipole moment matrices, $\Delta\mu^{\text{ad}}$, see eq. S2), charge differences (Δq_{ii} , in the adiabatic charge difference matrices, Δq^{ad} , see eq. S2), respectively. Moreover, we used NTOs to illustrate and verify the charge density distributions of these states. The dominant hole-electron NTO pair was mostly considered, especially with the global hybrid functionals, which in this study generally yielded the predominant NTO pair with a fraction (λ_{NTO}) larger than 0.9 for the electron transition in question (see Figure 3 in the main article and Figure S5 below). In the 4–7 -state schemes, higher-energy CT states (CT₂, CT₃, etc.) were manually selected and included in the $\Delta\mu^{\text{ad}}$ and Δq^{ad} matrices in addition to the GS, CT₁, and LE states. In the 11-state schemes, the GS and 10 lowest singlet excited states were used to form the diabatic states, which were then identified automatically by using the classification as proposed by Yang and Hsu¹⁰. In the GMH, typical local states (GS, LE, and local excitations within PC₇₁BM, i.e. LF) have small dipole moments¹⁰, whereas the dipole moments of the CT states should approach the ideal dipole moment defined as $\Delta\mu_{\text{if}}^{\text{id}} = eR_{\text{eD-eA}}$ ¹¹, where $R_{\text{eD-eA}}$ is the effective separation of the eD and eA sites. When $R_{\text{eD-eA}}$ is approximated as the distance between the mass centers of TQ and PC₇₁BM¹² (8.55 Å for T-series and 8.59 Å for Q-series), $\Delta\mu_{\text{if}}^{\text{id}}$ of 41.1 D for T-series and 41.3 D for Q-series are obtained. Yang et al have used¹⁰ half of $\Delta\mu_{\text{if}}^{\text{id}}$ as the threshold

when assigning the states as the local or CT states according to their eigenvalue in the diagonalized $\Delta\boldsymbol{\mu}$ matrix (obtained from eq. S2). However, we have used the threshold of 10.0 D for assigning the states, because in our case (the half of $\Delta\boldsymbol{\mu}_{if}^{ad}$ is 20.6 and 20.7 for T- and Q-series, respectively) there would have not been any CT states in some cases (the 2–4 -state GMH schemes with the LRC functionals). In FCD, Δq_{ii} of a CT state should be close to 2 or -2, whereas Δq_{ii} of a local state is close to zero. Like suggested by Yang et al¹⁰, we have used ± 1 as the threshold for Δq to assign the local and CT subspaces in the diagonalized $\Delta\mathbf{q}$ matrix (obtained from eq. S2).

Electronic coupling. Using the GMH^{11,13} and FCD¹⁴ schemes as implemented in Q-Chem 4.2,¹⁵ we calculated the adiabatic electronic ($\boldsymbol{\mu}_{ii}^{ad}$) and transition dipole moments ($\boldsymbol{\mu}_{ij}^{ad}$) (in GMH) and the charge differences (Δq_{ii}^{ad} and Δq_{ij}^{ad} , in FCD) for the GS and ten lowest singlet excited states. Although the Q-Chem software yields the H_{if} values directly during these calculations, only the ones obtained with the 2-state FCD scheme were used as such. The projections of the dipole moments calculated with the GMH scheme in Q-Chem were further used to calculate the GMH couplings (see below). In the GMH, which is a generalization from the Mulliken–Hush (MH) expression^{16–20}, the diabatic states localized at different sites (e.g. LE and CT states) are assumed to have a zero transition dipole moment ($\boldsymbol{\mu}_{if} = 0$) between them. Moreover, the diabatic states localized at the same sites have H_{if} of zero between them.^{11,13} The same assumption regarding H_{if} is made in FCD, i.e. that the transition densities (Δq_{if}) between the diabatic states localized at different sites are zero. We followed the approach proposed by Yang and Hsu¹⁰, which is based on the similar 3-state approaches^{21,22}, for assigning the local and CT states (see ‘Assignment of the states’ above) and calculating the H_{if} values with the multi-state (i.e. the number of states, $N \geq 3$) GMH and FCD schemes. The first step is to diagonalize the adiabatic dipole moment matrix ($\boldsymbol{\mu}^{ad}$) (or similarly the adiabatic charge difference matrix, $\Delta\mathbf{q}^{ad}$, in FCD) with a unitary transformation matrix \mathbf{U}_1 , which is composed of the eigenvectors of $\boldsymbol{\mu}^{ad}$ (or similarly to $\Delta\mathbf{q}^{ad}$):

$$U_1^T \boldsymbol{\mu}^{ad} U_1 = U_1^T \begin{pmatrix} \mu_{11} & \mu_{12} & \mu_{13} & \dots \\ \mu_{21} & \mu_{22} & \mu_{23} & \dots \\ \mu_{31} & \mu_{32} & \mu_{33} & \dots \\ \vdots & \vdots & \vdots & \ddots \end{pmatrix} U_1 = \begin{pmatrix} \mu_l & 0 & 0 & \dots \\ 0 & \mu_m & 0 & \dots \\ 0 & 0 & \mu_n & \dots \\ \vdots & \vdots & \vdots & \ddots \end{pmatrix} \quad (\text{S2})$$

Here, the diagonal elements, i.e. $\boldsymbol{\mu}_{ii}^{ad}$ are relative to the GS dipole moment. Applying the same transformation to the corresponding adiabatic Hamiltonian, i.e. the diagonal matrix \mathbf{E} of the adiabatic energy, yields the Hamiltonian (\mathbf{H}):

$$U_1^T \mathbf{E} U_1 = U_1^T \begin{pmatrix} E_1 & 0 & 0 & \dots \\ 0 & E_2 & 0 & \dots \\ 0 & 0 & E_3 & \dots \\ \vdots & \vdots & \vdots & \ddots \end{pmatrix} U_1 = \begin{pmatrix} H_{ll} & H_{lm} & H_{ln} & \dots \\ H_{ml} & H_{mm} & H_{mn} & \dots \\ H_{nl} & H_{nm} & H_{nn} & \dots \\ \vdots & \vdots & \vdots & \ddots \end{pmatrix} \quad (\text{S3})$$

In the limiting case of the 2-state schemes, the diabatic dipole moment matrix ($\boldsymbol{\mu}^{diab}$) (or similarly the diabatic charge difference matrix, $\Delta\mathbf{q}^{diab}$) and diabatic Hamiltonian (\mathbf{H}^{diab}) can be obtained already from eq. S2 and S3 (or from eq. S6 and S11). However, when more states are considered, i.e. in the multi-state schemes, there may exist several states localized on the same site, i.e. with the same nature,

and therefore \mathbf{H} should be re-diagonalized within the blocks of the same-site states. The states obtained in this manner are adiabatic within one block, but diabatic with respect to the states localized at different sites.¹⁰ Thus, the next step is to classify the states as the local states (LS, which includes GS, LE or LF states) or CT states according to their eigenvalues (see ‘Assignment of the states’ above) in diagonalized $\boldsymbol{\mu}$ (or $\Delta\mathbf{q}$) matrix (obtained from eq. S2). After this, \mathbf{H} (obtained from eq. S3) is re-diagonalized within each block (i.e. LS and CT) to define the \mathbf{H}^{diab} :

$$U_2^T \begin{pmatrix} H_{LS} & H_{LS,CT} \\ H_{CT,LS} & H_{CT} \end{pmatrix} U_2 = \begin{pmatrix} E_{LS} & H_{LS,CT} \\ H_{CT,LS} & E_{CT} \end{pmatrix} \quad (\text{S4})$$

where each bold letter refer to a matrix in the LS and CT subspaces defined by the subscript, \mathbf{E} is a diagonal matrix, and the final coupling values (H_{if}) are the corresponding matrix elements in $H_{LS,CT}$. Finally, $\boldsymbol{\mu}^{\text{diab}}$ (or similarly $\Delta\mathbf{q}^{\text{diab}}$) can be obtained by applying the same transformation U_2 to the diagonalized $\boldsymbol{\mu}$ (or similarly to $\Delta\mathbf{q}$) obtained from eq. S2:

$$U_2^T \begin{pmatrix} \mu_l & 0 & 0 & \dots \\ 0 & \mu_m & 0 & \dots \\ 0 & 0 & \mu_n & \dots \\ \vdots & \vdots & \vdots & \ddots \end{pmatrix} U_2 = \begin{pmatrix} \mu_{LS}^{\text{diab}} & 0 \\ 0 & \mu_{CT}^{\text{diab}} \end{pmatrix} \quad (\text{S5})$$

In the limiting 2-state GMH scheme^{11,13}, the coupling between two charge-localized states, i.e. diabatic states $|i\rangle$ and $|f\rangle$ is defined as

$$H_{if} = \frac{\mu_{12}\Delta E_{12}}{\Delta\mu_{if}^{\text{diab}}} = \frac{\mu_{12}\Delta E_{12}}{\sqrt{(\Delta\mu_{12})^2 + 4\mu_{12}^2}} \quad (\text{S6})$$

where diabatic \mathbf{H}_{if} and the difference of the diabatic state dipole moments ($\Delta\boldsymbol{\mu}_{if}^{\text{diab}}$) are expressed in adiabatic terms; $\boldsymbol{\mu}_{12}$ being the adiabatic transition dipole moment, ΔE_{12} ($= E_2 - E_1$) being the vertical excitation energy difference, and $\Delta\boldsymbol{\mu}_{12}$ ($= \boldsymbol{\mu}_1 - \boldsymbol{\mu}_2$) being the difference between the electronic dipole moments of the adiabatic states $|1\rangle$ and $|2\rangle$. In this study, the total values of $\boldsymbol{\mu}_{ij}$ employed in the 2- and multi-state GMH schemes are defined as

$$\mu_{ij} = \sqrt{(\mu_{x,ij})^2 + (\mu_{y,ij})^2 + (\mu_{z,ij})^2} \quad (\text{S7})$$

whereas $\Delta\boldsymbol{\mu}_{ij}$ are defined as

$$\Delta\mu_{ij} = \sqrt{(\mu_{x,i} - \mu_{x,j})^2 + (\mu_{y,i} - \mu_{y,j})^2 + (\mu_{z,i} - \mu_{z,j})^2} \quad (\text{S8})$$

In the GMH scheme, the dipole moment vectors are typically projected either on the direction defined by $\Delta\boldsymbol{\mu}_{12}$ (or the average of such differences in the multi-state case)^{11,13,22,23} or the CT vector¹², which is defined as the vector between the centers of mass of two molecules. Here, we have employed the

latter, i.e. the projections of the μ_{ii} and μ_{ij} along the CT vector defined as the vector connecting the mass centers of TQ and PC₇₁BM, i.e. $e\mathbf{R}_{eD-eA}$. The projected transition dipole moment vectors are

$$proj_{R_{eD-eA}} \mu_{ij} = \frac{(\mu_{ij} \cdot R_{eD-eA})}{|R_{eD-eA}|^2} R_{eD-eA} \quad (\text{S9})$$

The projections of the electronic dipole moments, μ_{ii} , are defined similarly.

The FCD scheme is similar to GMH, but instead of a dipole moment, a charge difference operator (Δq) is employed. The system is partitioned into two fragments corresponding to eD and eA, which are in our case TQ and PC₇₁BM, respectively. An adiabatic eD–eA charge difference matrix, $\Delta \mathbf{q}^{\text{ad}}$, is defined by its elements

$$\Delta q_{ij}^{\text{ad}} = \int_{r \in eD} \rho_{ij}(r) dr - \int_{r \in eA} \rho_{ij}(r) dr \quad (\text{S10})$$

where $\rho_{ij}(\mathbf{r})$ is the one-particle density (if $i = j$) for the diagonal elements $\Delta q_{ii}^{\text{ad}}$ and $\Delta q_{jj}^{\text{ad}}$ defined as the eD–eA charge differences in the adiabatic states $|i\rangle$ and $|j\rangle$, respectively, or the transition density for the off-diagonal terms $\Delta q_{ij}^{\text{ad}}$ (if $i \neq j$). For the 2-state FCD¹⁴, the coupling values are calculated with the following formulation:

$$H_{if} = \frac{|\Delta q_{12}| \Delta E_{12}}{\sqrt{(\Delta q_1 - \Delta q_2)^2 + 4\Delta q_{12}^2}} \quad (\text{S11})$$

In the FCD scheme, Q-Chem uses the Mulliken population analysis for determining the atomic charges of the atoms. The Mulliken population analysis is known to suffer from several problems, especially the equally divided off-diagonal elements of the population matrix to two atoms regardless of their electronegativities. However, as the total charges on two fragments are calculated in FCD, this problem can be expected to have only a minor effect here.²⁴

Reorganization energy. The reorganization energy is divided into the inner (λ_i) and outer (λ_s) contributions,

$$\lambda = \lambda_i + \lambda_s \quad (\text{S12})$$

The inner part of the reorganization energy originates from the changes in the eD and eA equilibrium geometries upon CT and it is determined as the difference between the energy of the reactants (or products) in the geometry of the products (or reactants) and that of their equilibrium geometry. These two ways results in the same value of λ_i only if the parabolas of the reactants and products have the same curvature, and as this is usually not the case, λ_i is estimated as the average of the reorganization

energies in the reactant and product states.²⁵ Thus, to calculate λ_i for ED, we have used the following equations^{25,26}:

$$\lambda_{i,ED} = (\lambda_{i1,ED} + \lambda_{i2,ED})/2 \quad (\text{S13})$$

$$\lambda_{i1,ED} = [E^{eD^*}(eD^+) + E^{eA}(eA^-)] - [E^{eD^*}(eD^*) + E^{eA}(eA)] \quad (\text{S14})$$

$$\lambda_{i2,ED} = [E^{eD^+}(eD^*) + E^{eA^-}(eA)] - [E^{eD^+}(eD^+) + E^{eA^-}(eA^-)] \quad (\text{S15})$$

where eD^* and eD^+ refer to the lowest singlet excited (S_1) and cationic states of the isolated TQ, respectively, and eA and eA^- refer to the neutral and anionic states of the isolated $PC_{71}BM$, respectively. The terms before the parentheses refer to the energies for the systems specified in the superscripts and the terms in the parentheses refer to the optimized geometries at which the SP energies are calculated. Similarly, we have calculated λ_i for CR with the following equations²⁷:

$$\lambda_{i,CR} = (\lambda_{i1,CR} + \lambda_{i2,CR})/2 \quad (\text{S16})$$

$$\lambda_{i1,CR} = [E^{eD^+}(eD) + E^{eA^-}(eA)] - [E^{eD^+}(eD^+) + E^{eA^-}(eA^-)] \quad (\text{S17})$$

$$\lambda_{i2,CR} = [E^{eD}(eD^+) + E^{eA}(eA^-)] - [E^{eD}(eD) + E^{eA}(eA)] \quad (\text{S18})$$

where eD refer to the GS energy of the neutral isolated TQ. The outer part of the reorganization energy originates from the changes in the electronic and nuclear polarizations and relaxation of the surrounding medium upon CT.²⁵ It can be estimated by using the classical dielectric continuum model developed by Marcus²⁸ with an assumption that the CT occurs in an isotropic dielectric environment. However, as the accurate prediction of λ_s is still rather difficult and it is highly affected by uncertainty of the calculated parameters²⁹, we chose to keep it as an adjusted parameter like in the previous studies^{30,31} and calculated the rate constants with λ_s of 0.1–0.75 eV.

Gibbs free energy difference. The Gibbs free energy difference (ΔG°) is the energy difference of the complexes in their final and initial states²⁵. Here we have used the Weller's equation for calculating ΔG° from the energies of TQ and $PC_{71}BM$, while taking the Coulombic attraction (ΔE_{coul}) between their charged states into account^{25,26}. For ED, ΔG° was calculated as

$$\Delta G_{ED}^\circ = E^{eD^+} + E^{eA^-} - E^{eD^*} - E^{eA} + \Delta E_{coul,ED} \quad (\text{S19})$$

where E^{eD^+} and E^{eD^*} are the total energies of the isolated TQ oligomer in the optimized geometries of the cation and of the S_1 state, respectively, E^{eA^-} and E^{eA} are the total energies of the isolated $PC_{71}M$ in the optimized geometries of the anion and the GS, respectively. The Coulomb energy is defined as

$$\Delta E_{coul,ED} = \sum_{eD^+} \sum_{eA^-} \frac{q_{eD^+} q_{eA^-}}{4\pi\epsilon_0\epsilon_s r_{eD^+eA^-}} - \sum_{eD^*} \sum_{eA} \frac{q_{eD^*} q_{eA}}{4\pi\epsilon_0\epsilon_s r_{eD^*eA}} \quad (S20)$$

where q and r are the atomic charges and the distance between them, respectively, the subscript defining the compound and its relevant state, ϵ_0 and ϵ_s are the vacuum permittivity and the relative permittivity of the medium (static dielectric constant), respectively. The partial atomic charges, i.e. q terms in eq. S20 were calculated using the Merz–Singh–Kollman (MK) scheme.^{32,33} The sums run over all atoms in each compound. Similarly, ΔG° for CR was calculated as

$$\Delta G_{CR}^\circ = E^{eD} + E^{eA} - E^{eD^+} - E^{eA^-} + \Delta E_{coul,CR} \quad (S21)$$

where the Coulomb energy is

$$\Delta E_{coul,CR} = \sum_{eD} \sum_{eA} \frac{q_{eD} q_{eA}}{4\pi\epsilon_0\epsilon_s r_{eDeA}} - \sum_{eD^+} \sum_{eA^-} \frac{q_{eD^+} q_{eA^-}}{4\pi\epsilon_0\epsilon_s r_{eD^+eA^-}} \quad (S22)$$

Results: additional details

Excited state characteristics of the isolated TQ and PC₇₁BM models and TQ–PC₇₁BM complexes

To select TQ–PC₇₁BM complexes with a representative length of TQ for the electronic coupling and CT rate calculations, we examined the effect of the length of TQ on the excited state properties of both the isolated TQ models and the TQ–PC₇₁BM complexes (Figure S1). Moreover, we compared the couplings of the selected complexes. The main findings related to similarities and differences in the excited state properties of the isolated compounds and complexes of the T- and Q-series are reported in the main article. Here, we compare the results obtained with two excited state methods TDDFT and TDA³⁴ and two functionals, the global hybrid functional B3LYP^{35,36} and the LRC functional CAM-B3LYP³⁷. For the isolated TQ and PC₇₁BM models (Table S2), TDDFT yields ca. 0.1–0.6 eV lower S_1 energies than TDA with both B3LYP and CAM-B3LYP. However, in the case of the complexes, both TD methods yield quite similar energies for the main excitation ($E_{vert,main}$, i.e. the excitation with the largest oscillator strength, see Tables S3 and S4). Moreover, TDDFT and TDA yield almost equal energies for the 10 lowest singlet excited states of the 3T4Q–PC₇₁BM and 3Q4T–PC₇₁BM complexes (Tables S5 and S6), with TDA energies being only 0.0–0.1 eV larger. For the complexes with TQ equal or longer than 3T2Q/3Q2T, TDDFT predicts the main excitation mainly as a pure LE state, while TDA tends to yield the main LE state with a mixed CT character, especially with CAM-B3LYP. Similarly, CAM-B3LYP predicts the main excitation as the LE state with a mixed LE and CT character in the complexes with 3T2Q and 3Q2T when using both TDDFT and TDA, and also in complexes with 3T4Q and 3Q4T when using TDA. The amount of CT in the lowest CT state (CT₁) is quite similar with both TDDFT and TDA when using the B3LYP functional (Table S3).

CAM-B3LYP predicts more differences in the amounts of CT between TDDFT and TDA (Table S4), TDA yielding more significant CT.

Table S1 Energies of the first singlet (S_1) excited states (in eV) of the isolated TQ and PC₇₁BM models^a calculated with TDDFT (TDA) using different functionals and the 6-31G* basis set.

Functional	T	T2Q	3T2Q	3T4Q	Q	Q2T	3Q2T	3Q4T	PC ₇₁ BM
B3LYP	5.94 (6.08)	2.63 (2.73)	2.14 (2.24)	1.92 (1.99)	3.56 (3.60)	2.57 (2.68)	2.14 (2.24)	1.91 (1.99)	2.03 (2.03)
CAM-B3LYP	6.03 (6.28)	3.15 (3.28)	2.64 (2.76)	2.43 (2.52)	3.85 (3.91)	3.08 (3.22)	2.64 (2.75)	2.43 (2.52)	2.27 (2.34)

^aTQ and PC₇₁BM models presented in Figure S1.

Table S2 Characteristics of the selected excited states of the TQ–PC₇₁BM complexes calculated with TDDFT (TDA) at the B3LYP/6-31G* level of theory.

Complex		T–	T2Q–	3T2Q–	3T4Q–	Q–	Q2T–	3Q2T–	3Q4T–
		PC ₇₁ BM							
The main excitation ^a	$E_{\text{vert,main}}$ (eV)	2.36 (2.39)	2.10 (2.10)	2.13 (2.21)	1.91 (1.98)	2.37 (2.42)	2.05 (2.05)	2.14 (2.21)	1.91 (1.98)
	State	S ₉ (S ₈)	S ₄ (S ₄)	S ₆ (S ₈)	S ₄ (S ₄)	S ₉ (S ₉)	S ₄ (S ₄)	S ₇ (S ₈)	S ₄ (S ₄)
	$\lambda_{\text{NTO,main}}$ ^b	0.46 (0.63)	0.82 (0.82)	0.68 (0.86)	0.97 (0.97)	0.45 (0.42)	0.91 (0.97)	0.45 (0.59)	0.97 (0.98)
	Nature ^c	LF (LF)	CT (CT)	LE (LE+CT)	LE (LE)	LF (LF)	PCT (PCT)	LE (LE)	LE (LE)
	Amount of CT (pp) ^d	0 (5)	71 (72)	4 (11)	5 (3)	0 (0)	92 (92)	2 (2)	1 (1)
	f_{main} ^e	0.0382 (0.0379)	0.0178 (0.0179)	0.5241 (0.7825)	1.4589 (1.8710)	0.0415 (0.0382)	0.0101 (0.0106)	0.4440 (0.6922)	1.4498 (1.8101)
The CT ₁ state ^f	E_{CT1} (eV)	-	1.96 (1.96)	1.70 (1.70)	1.61 (1.61)	-	1.91 (1.92)	1.69 (1.69)	1.58 (1.58)
	$\lambda_{\text{NTO,CT1}}$ ^b	-	0.96 (0.96)	1.00 (1.00)	1.00 (1.00)	-	0.99 (0.99)	1.00 (1.00)	1.00 (1.00)
	Amount of CT (pp) ^d	-	75 (75)	96 (96)	96 (96)	-	91 (92)	97 (97)	98 (98)
	f_{CT1} ^e	-	0.0053 (0.0054)	0.0129 (0.0122)	0.0322 (0.0274)	-	0.0025 (0.0026)	0.0072 (0.0067)	0.0148 (0.0128)

^aThe excitation with the largest oscillator strength. ^bFraction of the hole-electron pair to the given transition. ^cLF = local excitation within PC₇₁BM, LE = local excitation within TQ, CT = charge transfer from TQ to PC₇₁BM, PCT = pure CT, i.e. more than 90 percentage points (pp) charge density transferred from TQ to PC₇₁BM. ^dAmount of charge density transferred from TQ to PC₇₁BM in percentage points. ^eOscillator strength. ^fThe lowest CT state (CT₁) was the S₁ state for all the complexes.

Table S3 Characteristics of the selected excited states of the TQ–PC₇₁BM complexes calculated with TDDFT (TDA) at the CAM-B3LYP/6-31G* level of theory.

Complex		T– PC ₇₁ BM	T2Q– PC ₇₁ BM	3T2Q– PC ₇₁ BM	3T4Q– PC ₇₁ BM	Q– PC ₇₁ BM	Q2T– PC ₇₁ BM	3Q2T– PC ₇₁ BM	3Q4T– PC ₇₁ BM
The main excitation ^a	E _{vert,main} (eV)	2.74 (2.80)	2.74 (2.79)	2.59 (2.67)	2.41 (2.48)	2.73 (2.80)	2.74 (2.80)	2.60 (2.69)	2.42 (2.50)
	State	S ₇ (S ₆)	S ₆ (S ₆)	S ₃ (S ₄)	S ₂ (S ₂)	S ₆ (S ₆)	S ₆ (S ₆)	S ₃ (S ₄)	S ₂ (S ₂)
	λ _{NTO,main} ^b	0.79 (0.67)	0.76 (0.67)	0.85 (0.81)	0.83 (0.78)	0.76 (0.66)	0.78 (0.65)	0.83 (0.83)	0.84 (0.74)
	Nature ^c	LF (LF)	LF (LF)	LE+CT (LE+CT)	LE (LE+CT)	LF (LF)	LF (LF)	LE+CT (LE+CT)	LE (LE+CT)
	Amount of CT (pp) ^d	0 (0)	0 (0)	18 (42)	7 (14)	0 (0)	0 (0)	12 (42)	5 (12)
	f _{main} ^e	0.0461 (0.0569)	0.0421 (0.0524)	0.8260 (0.6347)	1.7524 (1.7050)	0.0480 (0.0629)	0.0453 (0.0581)	0.9181 (0.7218)	1.7957 (1.6261)
The CT state ^f	E _{CT} (eV)	-	-	2.74 (2.79)	2.67 ^g (2.69)	-	-	2.74 (2.77)	2.67 ^g (2.68)
	State	-	-	S ₇ (S ₇)	S ₅ ^g (S ₅)	-	-	S ₇ (S ₇)	S ₅ ^g (S ₅)
	λ _{NTO, CT₁} ^b	-	-	0.76 (0.64)	0.77 ^g (0.81)	-	-	0.75 (0.66)	0.78 ^g (0.89)
	Amount of CT (pp) ^d	-	-	11 (15)	38 ^g (67)	-	-	19 (48)	67 ^g (83)
	f _{CT} ^e	-	-	0.0542 (0.0823)	0.0431 ^g (0.1366)	-	-	0.0320 (0.1567)	0.0262 ^g (0.0933)

^aThe excitation with the largest oscillator strength. ^b Fraction of the hole-electron pair to the given transition. ^cLF = local excitation within PC₇₁BM, LE = local excitation within TQ, CT = charge transfer from TQ to PC₇₁BM. ^dAmount of charge density transferred from TQ to PC₇₁BM in percentage points. ^eOscillator strength. ^fWhen E_{vert,main} have a CT contribution, the characteristics of the second lowest CT state (CT₂) are reported for the CT state. ^gThe CT₁ state was considered.

Optimally tuned range separation parameters of the selected isolated TQ and PC₇₁BM models and TQ-PC₇₁BM complexes

Table S4 Optimally tuned (OT) range separation parameters (ω) of OT-BNL determined using the gap tuning procedures^a with the 6-31G* basis set.

Model	OT ω (bohr ⁻¹)
3T4Q	0.15
3Q4T	0.15
PC ₇₁ BM	0.18
TQ-PC ₇₁ BM	0.17

^aThe OT ω values of the isolated molecules were determined using the gap tuning procedure described in ref. 8 and 9. For TQ-PC₇₁BM complexes, eq. S1 was used.

Excitation energies of the 3T4Q-PC₇₁BM and 3Q4T-PC₇₁BM complexes

i) TDDFT in vacuum with the 6-31G* basis set

Table S5 Vertical excitation energies (in eV)^a calculated with TDDFT in vacuum using different functionals and the 6-31G* basis set.

Functional	Complex	S ₁	S ₂	S ₃	S ₄	S ₅	S ₆	S ₇	S ₈	S ₉	S ₁₀
B3LYP	3T4Q-PC ₇₁ BM	1.6096	1.6750	1.7513	1.9138	2.0301	2.0583	2.1398	2.1755	2.1868	2.1979
	3Q4T-PC ₇₁ BM	1.5744	1.6392	1.7129	1.9131	2.0286	2.0519	2.1387	2.1449	2.1518	2.1755
PBE0	3T4Q-PC ₇₁ BM	1.7035	1.7782	1.8489	2.0215	2.1138	2.1415	2.2335	2.2734	2.3023	2.3175
	3Q4T-PC ₇₁ BM	1.6720	1.7450	1.8139	2.0275	2.1153	2.1433	2.2333	2.2633	2.2746	2.2848
CAM-B3LYP	3T4Q-PC ₇₁ BM	2.2665	2.4056	2.4663	2.6301	2.6652	2.6836	2.7115	2.7412	2.767	2.7852
	3Q4T-PC ₇₁ BM	2.2712	2.4225	2.4667	2.6247	2.6652	2.6903	2.7066	2.7475	2.7618	2.7905
OT-BNL	3T4Q-PC ₇₁ BM	2.1086	2.1947	2.2273	2.3825	2.4084	2.4282	2.4645	2.5013	2.5293	2.5465
	3Q4T-PC ₇₁ BM	2.1144	2.208	2.2274	2.3833	2.4095	2.4426	2.4558	2.5132	2.5236	2.5509

^aRelative to the GS (S₀). These are the adiabatic values.

i) TDA in vacuum with the 6-31G* basis set

Table S6 Vertical excitation energies (in eV)^a calculated with TDA in vacuum using different functionals and the 6-31G* basis set.

Functional	Complex	S ₁	S ₂	S ₃	S ₄	S ₅	S ₆	S ₇	S ₈	S ₉	S ₁₀
B3LYP	3T4Q-PC ₇₁ BM	1.6109	1.6753	1.7525	1.9753	2.0313	2.0588	2.141	2.1765	2.1869	2.1983
	3Q4T-PC ₇₁ BM	1.5751	1.6394	1.7131	1.9774	2.0332	2.0625	2.1416	2.1450	2.1520	2.1833
PBE0	3T4Q-PC ₇₁ BM	1.7050	1.7785	1.8501	2.0848	2.1155	2.1421	2.2357	2.2752	2.3027	2.3192
	3Q4T-PC ₇₁ BM	1.6727	1.7451	1.8141	2.0865	2.1173	2.1446	2.2361	2.2633	2.2757	2.2856
CAM-B3LYP	3T4Q-PC ₇₁ BM	2.3313	2.4790	2.5167	2.6564	2.6888	2.7289	2.7364	2.7862	2.8130	2.8211
	3Q4T-PC ₇₁ BM	2.3356	2.4957	2.5188	2.6558	2.6793	2.7308	2.7377	2.7916	2.8127	2.8209
OT-BNL	3T4Q-PC ₇₁ BM	2.1531	2.2539	2.2820	2.4060	2.4329	2.4771	2.4840	2.5449	2.5679	2.5758
	3Q4T-PC ₇₁ BM	2.1595	2.2659	2.2900	2.4056	2.4239	2.4783	2.4840	2.5556	2.5685	2.5783

^aRelative to the GS (S₀). These are the adiabatic values.

ii) TDDFT in vacuum with the 6-31G and 6-31+G* basis sets**

Table S7 Vertical excitation energies (in eV)^a calculated with TDDFT in vacuum using different functionals and the 6-31G** basis set.

Functional	Complex	S ₁	S ₂	S ₃	S ₄	S ₅	S ₆	S ₇	S ₈	S ₉	S ₁₀
B3LYP	3T4Q-PC ₇₁ BM	1.6131	1.6793	1.7549	1.9089	2.0149	2.0299	2.1318	2.1576	2.188	2.1967
	3Q4T-PC ₇₁ BM	1.5790	1.6443	1.7175	1.9058	2.0175	2.0339	2.1337	2.1486	2.1552	2.166
PBE0	3T4Q-PC ₇₁ BM	1.7060	1.7815	1.8515	2.0184	2.0939	2.1134	2.2248	2.2568	2.2948	2.3041
	3Q4T-PC ₇₁ BM	1.6755	1.7491	1.8175	2.0149	2.0958	2.116	2.227	2.2614	2.2672	2.2851
CAM-B3LYP	3T4Q-PC ₇₁ BM	2.2759	2.4158	2.4698	2.6267	2.6699	2.6731	2.7162	2.7372	2.7700	2.7926
	3Q4T-PC ₇₁ BM	2.2801	2.4294	2.4727	2.627	2.6689	2.6766	2.7132	2.7415	2.7677	2.795
OT-BNL	3T4Q-PC ₇₁ BM	2.1065	2.1985	2.2308	2.3834	2.4129	2.4294	2.4678	2.5089	2.5275	2.5454
	3Q4T-PC ₇₁ BM	2.1121	2.2137	2.2317	2.3853	2.4153	2.4397	2.4626	2.517	2.5253	2.5509

^aRelative to the GS (S₀). These are the adiabatic values.

Table S8 Vertical excitation energies (in eV)^a calculated with TDDFT in vacuum using different functionals and the 6-31+G* basis set.

Functional	Complex	S ₁	S ₂	S ₃	S ₄	S ₅	S ₆	S ₇	S ₈	S ₉	S ₁₀
B3LYP	3T4Q-PC ₇₁ BM	1.4578	1.5279	1.6015	1.8532	1.9980	2.0083	2.0167	2.0469	2.1073	2.1159

^aRelative to the GS (S₀). These are the adiabatic values.

iii) TDDFT in 1,2-DCB and blend with the 6-31G* basis set

Table S9 Vertical excitation energies (in eV)^a calculated with TDDFT in 1,2-DCB using different functionals and the 6-31G* basis set.

Functional	Complex	S ₁	S ₂	S ₃	S ₄	S ₅	S ₆	S ₇	S ₈	S ₉	S ₁₀
B3LYP	3T4Q-PC ₇₁ BM	1.6519	1.7271	1.7948	1.8782	1.9908	2.023	2.1284	2.1686	2.1874	2.2291
	3Q4T-PC ₇₁ BM	1.6365	1.7111	1.7811	1.8733	1.9904	2.0253	2.1285	2.1718	2.1868	2.2016
PBE0	3T4Q-PC ₇₁ BM	1.7329	1.8208	1.8825	1.9885	2.0729	2.1007	2.2218	2.2712	2.2848	2.3346
	3Q4T-PC ₇₁ BM	1.7198	1.8065	1.8701	1.9848	2.072	2.1006	2.2221	2.276	2.2825	2.3153
CAM-B3LYP	3T4Q-PC ₇₁ BM	2.2637	2.3743	2.4402	2.6132	2.6662	2.6845	2.7171	2.7223	2.7684	2.7940
	3Q4T-PC ₇₁ BM	2.2683	2.389	2.4409	2.6110	2.6666	2.6919	2.7155	2.7281	2.7687	2.7974
OT-BNL	3T4Q-PC ₇₁ BM	2.0961	2.1728	2.2045	2.3745	2.4204	2.4286	2.4836	2.4969	2.523	2.5465
	3Q4T-PC ₇₁ BM	2.1015	2.1889	2.2044	2.3727	2.423	2.4394	2.4835	2.4976	2.525	2.5502

^aRelative to the GS (S₀). These are the adiabatic values.

Table S10 Vertical excitation energies (in eV)^a calculated with TDDFT in blend using different functionals and the 6-31G* basis set.

Functional	Complex	S ₁	S ₂	S ₃	S ₄	S ₅	S ₆	S ₇	S ₈	S ₉	S ₁₀
B3LYP	3T4Q-PC ₇₁ BM	1.6350	1.7082	1.7759	1.852	1.9973	2.0207	2.1282	2.1636	2.1872	2.2101
	3Q4T-PC ₇₁ BM	1.6174	1.689	1.7601	1.8442	1.9978	2.024	2.1285	2.1671	2.1866	2.1938
PBE0	3T4Q-PC ₇₁ BM	1.719	1.804	1.8659	1.9615	2.0785	2.0994	2.2209	2.2649	2.2844	2.3195
	3Q4T-PC ₇₁ BM	1.7039	1.7865	1.8517	1.9547	2.0786	2.0996	2.2214	2.27	2.2825	2.2995
CAM-B3LYP	3T4Q-PC ₇₁ BM	2.2635	2.3474	2.4401	2.6125	2.6598	2.6757	2.7153	2.7185	2.7583	2.7892
	3Q4T-PC ₇₁ BM	2.2679	2.3609	2.4418	2.6108	2.6603	2.6846	2.7121	2.7214	2.7574	2.7944
OT-BNL	3T4Q-PC ₇₁ BM	2.0968	2.1483	2.2045	2.3751	2.4172	2.4214	2.4761	2.4926	2.514	2.5434
	3Q4T-PC ₇₁ BM	2.1021	2.1626	2.2057	2.3738	2.4204	2.4311	2.4756	2.4938	2.5162	2.5481

^aRelative to the GS (S₀). These are the adiabatic values.

Adiabatic and diabatic dipole moments and charge differences of the CT₁ and LE states

i) TDDFT in vacuum, 1,2-DCB, and blend with the 6-31G* basis set

Table S11 Adiabatic and diabatic electric dipole moments ($\Delta\mu_{ii}^{\text{ad}}$ and $\Delta\mu^{\text{diab}}$)^a and charge differences ($\Delta q_{ii}^{\text{ad}}$ and Δq^{diab}) for the CT₁ and LE states of the studied TQ-PC₇₁BM complexes calculated with the 11-state GMH and FCD schemes^b using different functionals and the 6-31G* basis set.

Scheme		GMH				FCD			
Functional	Complex	$\Delta\mu_{CT_1}^{\text{ad}}$	$\Delta\mu_{CT_1}^{\text{diab}}$	$\Delta\mu_{LE}^{\text{ad}}$	$\Delta\mu_{LE}^{\text{diab}}$	$\Delta q_{CT_1}^{\text{ad}}$	$\Delta q_{CT_1}^{\text{diab}}$	$\Delta q_{LE}^{\text{ad}}$	$\Delta q_{LE}^{\text{diab}}$
B3LYP	3T4Q-PC ₇₁ BM	31.0 (29.0) [29.1]	31.2 (29.6) [29.6]	1.1 (4.6) [5.3]	0.3 (0.4) [0.5]	1.9 (1.9) [1.9]	2.0 (2.0) [2.0]	0.1 (0.3) [0.3]	0.0 (0.0) [0.0]
	3Q4T-PC ₇₁ BM	31.4 (30.0) [30.2]	31.4 (30.5) [30.7]	0.2 (0.9) [1.0]	0.1 (0.0) [0.1]	2.0 (2.0) [2.0]	2.0 (2.0) [2.0]	0.0 (0.1) [0.1]	0.0 (0.0) [0.0]
PBE0	3T4Q-PC ₇₁ BM	29.9 (28.4) [28.5]	30.2 (29.2) [29.2]	1.4 (3.6) [4.3]	0.2 (0.3) [0.4]	1.9 (1.9) [1.9]	2.0 (2.0) [2.0]	0.1 (0.2) [0.3]	0.0 (0.0) [0.0]
	3Q4T-PC ₇₁ BM	30.5 (29.3) [29.5]	30.7 (29.9) [30.0]	0.1 (0.9) [1.0]	0.3 (0.0) [0.1]	2.0 (2.0) [1.9]	2.0 (2.0) [2.0]	0.0 (0.1) [0.1]	0.0 (0.0) [0.0]
CAM-B3LYP	3T4Q-PC ₇₁ BM	12.5 (8.2) [9.6]	26.6 (25.6) [24.5]	1.3 (0.9) [0.9]	0.6 (0.4) [0.3]	0.7 (0.6) [0.6]	1.9 (1.8) [1.7]	0.1 (0.1) [0.1]	0.0 (0.0) [0.0]
	3Q4T-PC ₇₁ BM	16.6 (7.9) [10.3]	27.9 (27.1) [26.7]	0.8 (0.5) [0.5]	0.3 (0.1) [0.1]	1.1 (0.6) [0.7]	1.9 (1.9) [1.9]	0.1 (0.1) [0.0]	0.0 (0.0) [0.0]
OT-BNL	3T4Q-PC ₇₁ BM	11.3 (7.9) [8.2]	24.5 (22.7) [23.2]	1.7 (1.2) [1.2]	0.3 (0.3) [0.7]	0.7 (0.5) [0.5]	1.8 (1.6) [1.6]	0.2 (0.1) [0.1]	0.0 (0.0) [0.0]
	3Q4T-PC ₇₁ BM	15.9 (9.0) [10.9]	26.3 (25.3) [25.4]	0.6 (0.2) [0.7]	0.5 (0.6) [0.3]	1.1 (0.6) [0.7]	1.9 (1.9) [1.9]	0.1 (0.1) [0.1]	0.0 (0.0) [0.0]

^aRelative to the GS. ^bValues calculated in vacuum, 1,2-DCB (in parentheses), and blend (in brackets).

i) **TDDFT in vacuum with the 6-31G** and 6-31+G* basis sets**

Table S12 Adiabatic and diabatic electric dipole moments ($\Delta\mu_{ii}^{\text{ad}}$ and $\Delta\mu^{\text{diab}}$)^a and charge differences ($\Delta q_{ii}^{\text{ad}}$ and Δq^{diab}) for the CT₁ and LE states of the studied complexes calculated with the 11-state GMH and FCD schemes^b using TDDFT the 6-31G** and 6-31+G*^c (in parentheses) basis sets.

Scheme		GMH				FCD			
Functional	Complex	$\Delta\mu_{\text{CT}_1}^{\text{ad}}$	$\Delta\mu_{\text{CT}_1}^{\text{diab}}$	$\Delta\mu_{\text{LE}}^{\text{ad}}$	$\Delta\mu_{\text{LE}}^{\text{diab}}$	$\Delta q_{\text{CT}_1}^{\text{ad}}$	$\Delta q_{\text{CT}_1}^{\text{dia}}$ b	$\Delta q_{\text{LE}}^{\text{ad}}$	$\Delta q_{\text{LE}}^{\text{diab}}$
B3LYP	3T4Q-PC ₇₁ BM	30.9	30.9	1.2	0.3	1.9 (1.6)	2.0 (1.6)	0.1 (0.3)	0.0 (0.4)
	3Q4T-PC ₇₁ BM	31.4	31.5	0.2	0.2	2.0	2.0	0.0	0.0
PBE0	3T4Q-PC ₇₁ BM	29.9	30.1	1.4	0.2	1.9	2.0	0.1	0.0
	3Q4T-PC ₇₁ BM	30.4	30.6	0.1	0.3	2.0	2.0	0.0	0.0
CAM-B3LYP	3T4Q-PC ₇₁ BM	12.7	26.8	1.4	0.5	0.8	1.9	0.1	0.0
	3Q4T-PC ₇₁ BM	15.9	27.9	0.8	0.8	1.1	1.9	0.1	0.0
OT-BNL	3T4Q-PC ₇₁ BM	11.2	24.4	1.5	0.2	0.7	1.7	0.2	0.0
	3Q4T-PC ₇₁ BM	15.8	26.1	0.4	0.9	1.1	1.9	0.1	0.0

^aRelative to the GS. ^bValues calculated in vacuum. ^cOnly with B3LYP for 3T4Q-PC₇₁BM.

i) **TDA in vacuum with the 6-31G* basis set**

Table S13 Adiabatic and diabatic electric dipole moments ($\Delta\mu_{ii}^{\text{ad}}$ and $\Delta\mu^{\text{diab}}$)^a and charge differences ($\Delta q_{ii}^{\text{ad}}$ and Δq^{diab}) for the CT₁ and LE states of the studied complexes calculated with the 11-state GMH and FCD schemes^b using TDA with the 6-31G*basis set.

Scheme		GMH				FCD			
Functional	Complex	$\Delta\mu_{\text{CT}_1}^{\text{ad}}$	$\Delta\mu_{\text{CT}_1}^{\text{diab}}$	$\Delta\mu_{\text{LE}}^{\text{ad}}$	$\Delta\mu_{\text{LE}}^{\text{diab}}$	$\Delta q_{\text{CT}_1}^{\text{a}}$ d	$\Delta q_{\text{CT}_1}^{\text{diab}}$	$\Delta q_{\text{LE}}^{\text{ad}}$	$\Delta q_{\text{LE}}^{\text{diab}}$
B3LYP	3T4Q-PC ₇₁ BM	31.3	31.4	0.6	0.4	2.0	2.0	0.1	0.0
	3Q4T-PC ₇₁ BM	31.6	31.6	0.4	0.1	2.0	2.0	0.0	0.0
PBE0	3T4Q-PC ₇₁ BM	30.2	30.3	0.9	0.2	2.0	2.0	0.1	0.0
	3Q4T-PC ₇₁ BM	30.6	30.7	0.1	0.2	2.0	2.0	0.0	0.0
CAM-B3LYP	3T4Q-PC ₇₁ BM	17.0	27.0	2.0	0.1	1.2	1.9	0.2	0.0
	3Q4T-PC ₇₁ BM	20.9	28.1	1.0	0.9	1.5	1.9	0.2	0.0
OT-BNL	3T4Q-PC ₇₁ BM	13.7	14.0	1.5	1.5	0.9	1.8	0.2	0.0
	3Q4T-PC ₇₁ BM	18.7	26.7	0.3	0.6	1.4	1.9	0.1	0.0

^aRelative to the GS. ^bValues calculated in vacuum.

NTOs of the 3T4Q–PC₇₁BM complex

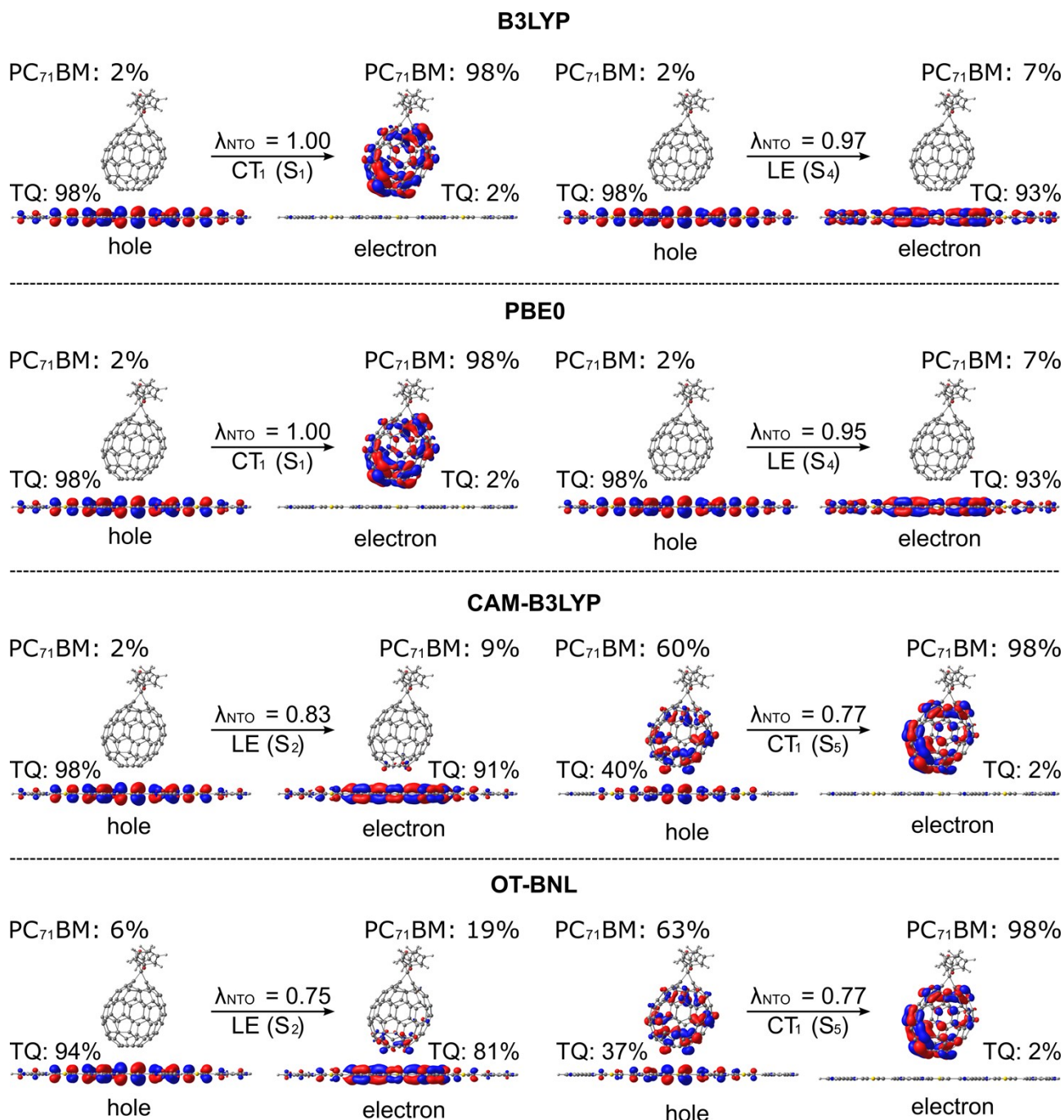


Figure S2 NTOs (the main pair) corresponding to the CT₁ and LE states of the 3T4Q–PC₇₁BM complex calculated with TDDFT using different functionals and 6-31G* basis set (isodensity contour = 0.025). The contributions (%) of TQ and PC₇₁BM to the NTOs and contributions (λ_{NTO}) of the NTO pair to the particular excitation are also presented.

Electronic couplings of 3T4Q-PC₇₁BM and 3Q4T-PC₇₁BM

i) Electronic couplings in vacuum with TDDFT and the 6-31G* basis set

Table S14 Electronic couplings (in meV) for the ED and CR processes of 3T4Q-PC₇₁BM calculated with TDDFT in vacuum using the GMH and FCD schemes with different number of the states (2–11) together with the different functionals and the 6-31G* basis set.

Scheme	B3LYP		PBE0		CAM-B3LYP		OT-BNL	
	ED	CR	ED	CR	ED	CR	ED	CR
2GMH	41.5	46.6	46.6	51	72.1	74	76.8	113.8
3GMH	41.7	50.8	46.8	56.1	72.6	108.6	77.2	137.8
4GMH	40.2	51.3	46.0	56.3	71.9	74.4	74.4	107.7
5GMH	38.3	47.8	43.5	51.8	-	-	-	-
6GMH	37.1	46.3	42.5	50.2	-	-	-	-
7GMH	36.8	45.3	-	-	-	-	-	-
11GMH	36.3	45.3	42.7	50.2	49.0	118.5	48.5	141.8
2FCD	38.4	44.0	42.7	46.4	82.7	122.2	82.7	138.9
3FCD	38.4	43.0	42.7	45.2	82.7	106.6	82.7	111.0
4FCD	37.7	43.0	42.2	45.3	69.2	75.5	70.7	83.0
5FCD	36.5	46.1	40.7	48.9	-	-	-	-
6FCD	36.9	46.4	40.8	48.8	-	-	-	-
7FCD	36.8	46.0	-	-	-	-	-	-
11FCD	37.3	46.3	41.7	48.8	59.7	80.5	65.5	88.1

Table S15 Electronic couplings (in meV) for the ED and CR processes of 3Q4T-PC₇₁BM calculated with TDDFT in vacuum using the GMH and FCD schemes with different number of the states (2–11) together with the different functionals and the 6-31G* basis set.

Scheme	B3LYP		PBE0		CAM-B3LYP		OT-BNL	
	ED	CR	ED	CR	ED	CR	ED	CR
2GMH	21.6	27.9	30.4	30.4	50.8	2.8	56.0	24.6
3GMH	22.0	31.0	30.6	34.3	51.0	33.9	52.9	54.8
4GMH	21.9	30.9	30.6	34.0	51.7	27.8	49.3	48.3
5GMH	21.9	30.8	30.5	33.7	-	-	-	-
6GMH	21.6	30.8	30.2	33.4	-	-	-	-
7GMH	21.4	30.4	30.1	33.6	-	-	-	-
8GMH	-	-	30.2	31.8	-	-	-	-
11GMH	21.3	30.4	30.4	31.6	35.2	63.6	33.2	92.4
2FCD	23.1	25.2	26.7	26.6	54.2	48.4	52.5	51.3
3FCD	23.1	25.2	26.7	26.4	54.2	45.9	52.5	47.7
4FCD	23	25.2	26.6	26.5	48.6	34.9	48.0	35.9
5FCD	22.9	25.7	26.5	27.1	-	-	-	-
6FCD	22.9	25.8	26.4	27.0	-	-	-	-
7FCD	22.9	26.1	26.6	25.6	-	-	-	-
8FCD	-	-	26.6	27.0	-	-	-	-
11FCD	23.1	25.7	26.8	27.0	43.5	39.1	44.8	44.1

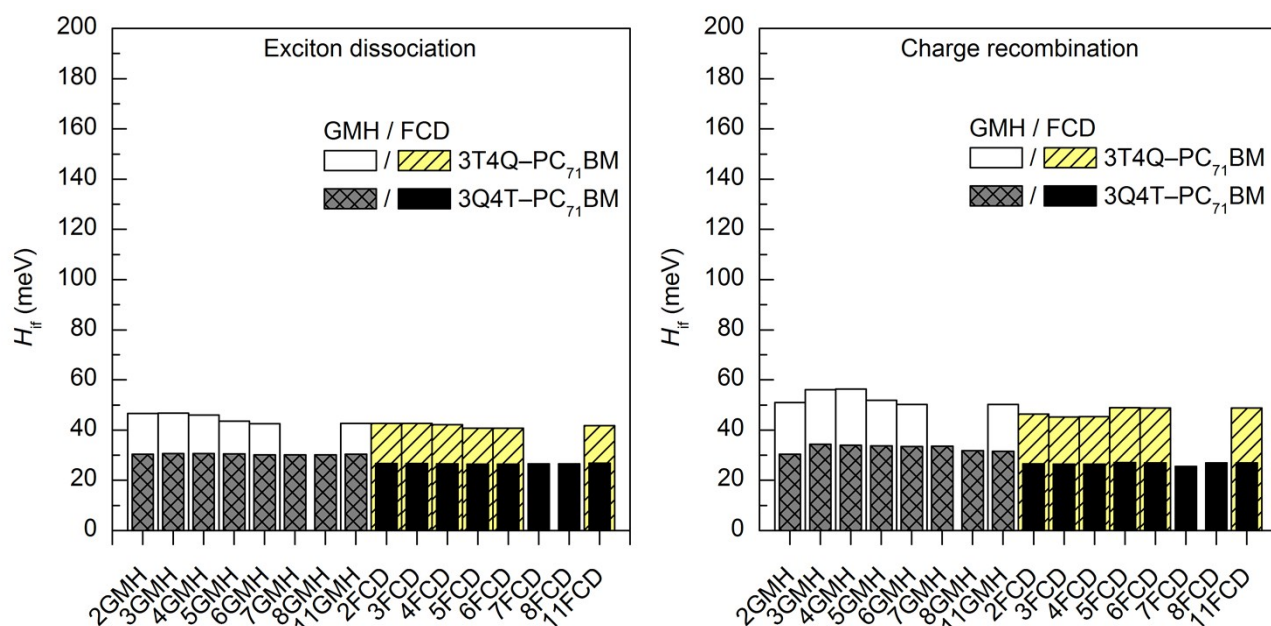


Figure S3 Electronic coupling values of the studied TQ-PC₇₁BM complexes calculated with TDDFT at the PBE0/6-31G* level of theory using either the GMH and FCD schemes with different number of states (2–11).

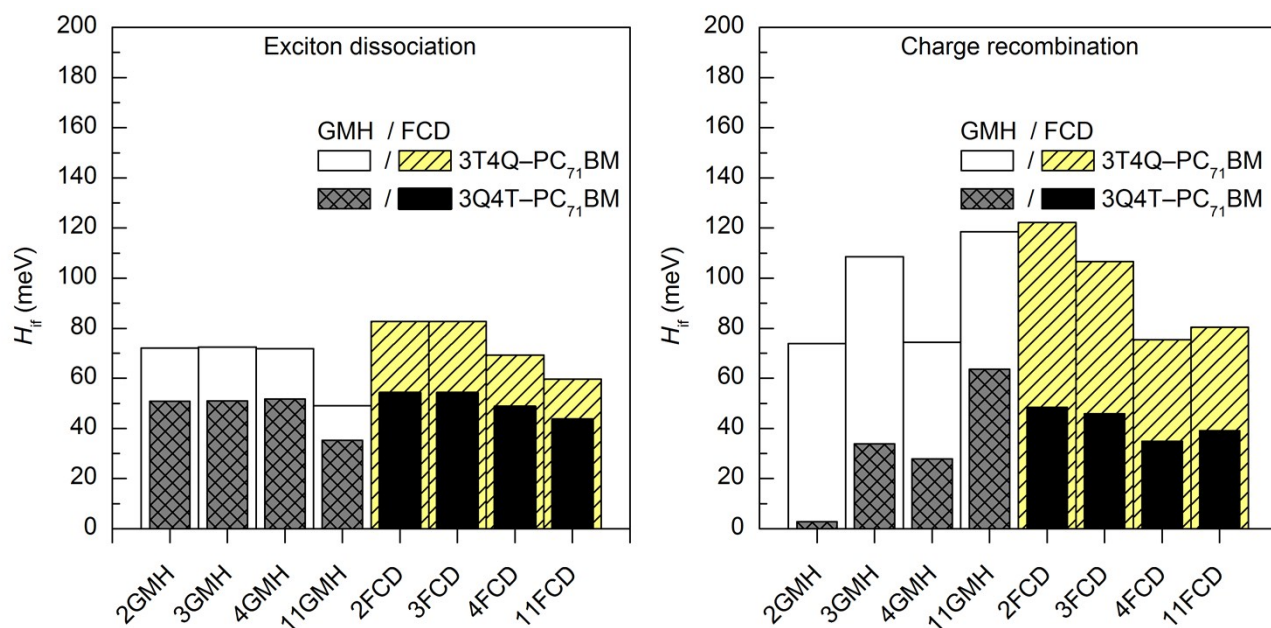


Figure S4 Electronic coupling values of the studied TQ-PC₇₁BM complexes calculated with TDDFT at the CAM-B3LYP/6-31G* level of theory using either the GMH and FCD schemes with different number of states (2–11).

i) Electronic couplings in vacuum with TDA and the 6-31G* basis set

Table S16 Electronic couplings (in meV) for the ED and CR processes of the studied complexes calculated with TDA in vacuum using the 11-state GMH and FCD schemes and the 6-31G* basis set.

Complex	Scheme	B3LYP		PBE0		CAM-B3LYP		OT-BNL	
		ED	CR	ED	CR	ED	CR	ED	CR
3T4Q-PC ₇₁ BM	11GMH	36.2	46.6	44.2	51.6	51.3	137.8	5.3	171.2
	11FCD	36.1	46.4	40.9	48.9	62.0	83.5	53.7	86.4
3Q4T-PC ₇₁ BM	11GMH	25.5	30.3	29.6	31.3	37.8	112.1	38.8	128.7
	11FCD	21.3	25.7	24.9	27.0	46.4	43.4	35.3	44.2

ii) Electronic couplings in vacuum with TDDFT and the 6-31G and 6-31+G* basis sets**

Table S17 Electronic couplings (in meV) for the ED and CR processes of 3T4Q-PC₇₁BM calculated with TDDFT in vacuum using the 11-state GMH and FCD schemes together with the different functionals and the 6-31G** or 6-31+G* basis sets.

Scheme	Basis set	B3LYP		PBE0		CAM-B3LYP		OT-BNL	
		ED	CR	ED	CR	ED	CR	ED	CR
11GMH	6-31G**	36.4	47.1	42.9	50.3	49.2	143.7	48.6	160.4
11FCD	6-31G**	37.6	46.3	41.7	48.9	60.9	83.4	70.0	89.6
	6-31+G*	39.1	46.9	-	-	-	-	-	-

Table S18 Electronic couplings (in meV) for the ED and CR processes of 3Q4T-PC₇₁BM calculated with TDDFT in vacuum using the 11-state GMH and FCD schemes together with the different functionals and the 6-31G** basis set.

Scheme	B3LYP		PBE0		CAM-B3LYP		OT-BNL	
	ED	CR	ED	CR	ED	CR	ED	CR
11GMH	25.6	30.9	29.4	31.4	37.6	109.2	32.7	114.7
11FCD	23.3	25.8	26.5	27.0	45.5	40.2	45.9	44.3

i) Electronic couplings in different environments with TDDFT and the 6-31G* basis set

Table S19 Electronic couplings (in meV) for the ED and CR processes of 3T4Q-PC₇₁BM calculated with TDDFT in different environments using the GMH and FCD schemes with 11 states together with the different functionals and the 6-31G* basis set.

Scheme	Medium	B3LYP		PBE0		CAM-B3LYP		OT-BNL	
		ED	CR	ED	CR	ED	CR	ED	CR
11GMH	vacuum	36.3	45.3	42.7	50.2	49.0	118.5	48.5	141.8
	1,2-DCB	36.6	50.1	43.8	53.7	55.5	180.1	44.1	203.9
	blend	34.6	49.3	41.8	53.4	56.7	168.8	54.5	252.0
11FCD	vacuum	37.3	46.3	41.7	48.8	59.7	80.5	65.5	88.1
	1,2-DCB	41.9	50.3	45.6	52.0	63.5	87.9	68.9	110.2
	blend	41.8	50.2	45.5	51.9	63.1	89.5	69.1	95.8

Table S20 Electronic couplings (in meV) for the ED and CR processes of 3Q4T-PC₇₁BM calculated with TDDFT in different environments using the GMH and FCD schemes with 11 states together with the different functionals and the 6-31G* basis set.

Scheme	Medium	B3LYP		PBE0		CAM-B3LYP		OT-BNL	
		ED	CR	ED	CR	ED	CR	ED	CR
11GMH	vacuum	21.3	30.4	30.4	31.6	35.2	63.6	33.2	92.4
	ODCB	31.0	38.4	35.0	42.7	43.4	102.3	29.5	149.9
	blend	30.4	38.2	34.5	42.2	43.9	124.1	38.7	121.9
11FCD	vacuum	23.1	25.7	26.8	27.0	43.5	39.1	44.8	44.1
	ODCB	29.2	28.0	32.5	29.0	49.9	41.7	52.2	47.1
	blend	29.4	27.7	32.6	28.6	49.4	41.6	48.3	47.3

Bond length alternations of 3T4Q and 3Q4T

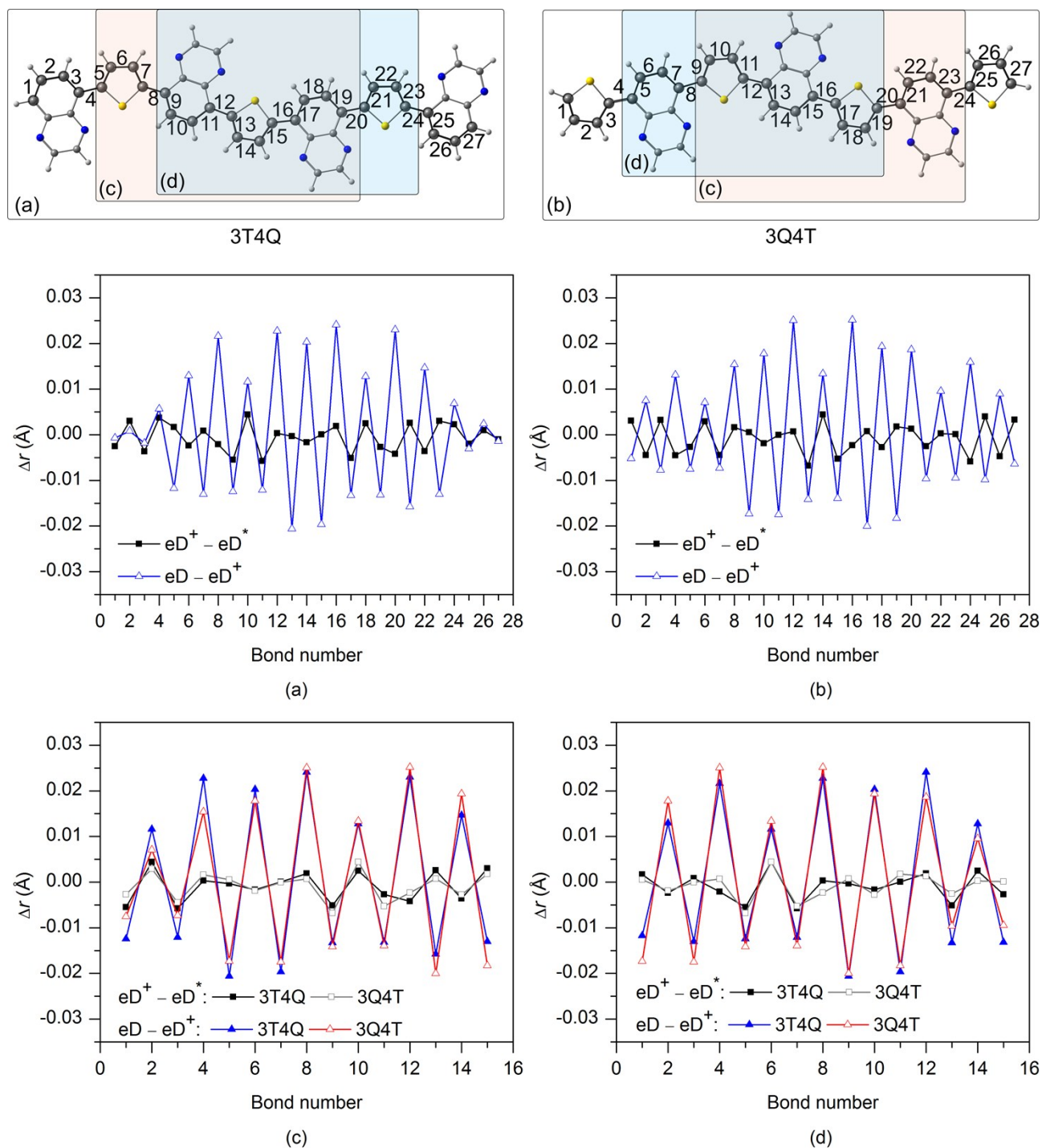


Figure S5 Changes in the bond lengths (Δr) of the whole backbones of (a) 3T4Q and (b) 3Q4T and of (c) & (d) two different middle parts of the molecules during the $eD^+ \rightarrow eD^+$ and $eD^+ \rightarrow eD$ transitions. The bond numbers for the whole backbones are defined along the numbered conjugation paths marked in the structures, which are presented above the graphs. Two different middle parts of the oligomers have also been considered to directly compare the changes in the similar parts of the molecules.

References

- 1 R. Baer and D. Neuhauser, *Phys. Rev. Lett.*, 2005, **94**, 043002.
- 2 E. Livshits and R. Baer, *Phys. Chem. Chem. Phys.*, 2007, **9**, 2932–2941.
- 3 T. Stein, L. Kronik and R. Baer, *J. Am. Chem. Soc.*, 2009, **131**, 2818–2820.
- 4 T. Stein, L. Kronik and R. Baer, *J. Chem. Phys.*, 2009, **131**, 244119.
- 5 B. Yang, Y. Yi, C.-R. Zhang, S. G. Aziz, V. Coropceanu and J.-L. Brédas, *J. Phys. Chem. C*, 2014, **118**, 27648–27656.
- 6 C.-R. Zhang, J. S. Sears, B. Yang, S. G. Aziz, V. Coropceanu and J.-L. Brédas, *J. Chem. Theory Comput.*, 2014, **10**, 2379–2388.
- 7 T. Kastinen, M. Niskanen, C. Risko, O. Cramariuc and T. I. Hukka, *Phys. Chem. Chem. Phys.*, 2016, **18**, 27654–27670.
- 8 T. Stein, H. Eisenberg, L. Kronik and R. Baer, *Phys. Rev. Lett.*, 2010, **105**, 266802.
- 9 S. Refaely-Abramson, R. Baer and L. Kronik, *Phys. Rev. B*, 2011, **84**, 075144.
- 10 C.-H. Yang and C.-P. Hsu, *J. Chem. Phys.*, 2013, **139**, 154104.
- 11 R. J. Cave and M. D. Newton, *Chem. Phys. Lett.*, 1996, **249**, 15–19.
- 12 C. Butchosa, S. Simon, L. Blancafort and A. Voityuk, *J. Phys. Chem. B*, 2012, **116**, 7815–7820.
- 13 R. J. Cave and M. D. Newton, *J. Chem. Phys.*, 1997, **106**, 9213–9226.
- 14 A. A. Voityuk and N. Rösch, *J. Chem. Phys.*, 2002, **117**, 5607–5616.
- 15 Y. Shao, Z. Gan, E. Epifanovsky, A. T. B. Gilbert, M. Wormit, J. Kussmann, A. W. Lange, A. Behn, J. Deng, X. Feng, D. Ghosh, M. Goldey, P. R. Horn, L. D. Jacobson, I. Kaliman, R. Z. Khaliullin, T. Kuš, A. Landau, J. Liu, E. I. Proynov, Y. M. Rhee, R. M. Richard, M. A. Rohrdanz, R. P. Steele, E. J. Sundstrom, H. L. Woodcock III, P. M. Zimmerman, D. Zuev, B. Albrecht, E. Alguire, B. Austin, G. J. O. Beran, Y. A. Bernard, E. Berquist, K. Brandhorst, K. B. Bravaya, S. T. Brown, D. Casanova, C.-M. Chang, Y. Chen, S. H. Chien, K. D. Closser, D. L. Crittenden, M. Diedenhofen, R. A. DiStasio, H. Do, A. D. Dutoi, R. G. Edgar, S. Fatehi, L. Fusti-Molnar, A. Ghysels, A. Golubeva-Zadorozhnaya, J. Gomes, M. W. D. Hanson-Heine, P. H. P. Harbach, A. W. Hauser, E. G. Hohenstein, Z. C. Holden, T.-C. Jagau, H. Ji, B. Kaduk, K. Khistyayev, J. Kim, J. Kim, R. A. King, P. Klunzinger, D. Kosenkov, T. Kowalczyk, C. M. Krauter, K. U. Lao, A. D. Laurent, K. V. Lawler, S. V. Levchenko, C. Y. Lin, F. Liu, E. Livshits, R. C. Lochan, A. Luenser, P. Manohar, S. F. Manzer, S.-P. Mao, N. Mardirossian, A. V. Marenich, S. A. Maurer, N. J. Mayhall, E. Neuscamman, C. M. Oana, R. Olivares-Amaya, D. P. O’Neill, J. A. Parkhill, T. M. Perrine, R. Peverati, A. Prociuk, D. R. Rehn, E. Rosta, N. J. Russ, S. M. Sharada, S. Sharma, D. W. Small, A. Sodt, T. Stein, D. Stück, Y.-C. Su, A. J. W. Thom, T. Tsuchimochi, V. Vanovschi, L. Vogt, O. Vydrov, T. Wang, M. A. Watson, J. Wenzel, A. White, C. F. Williams, J. Yang, S. Yeganeh, S. R. Yost, Z.-Q. You, I. Y. Zhang, X. Zhang, Y. Zhao, B. R. Brooks, G. K. L. Chan, D. M. Chipman, C. J. Cramer, W. A. Goddard, M. S. Gordon, W. J. Hehre, A. Klamt, H. F. Schaefer, M. W. Schmidt, C. D. Sherrill, D. G. Truhlar, A. Warshel, X. Xu, A. Aspuru-Guzik, R. Baer, A. T. Bell, N. A. Besley, J.-D. Chai, A. Dreuw, B. D. Dunietz, T. R. Furlani, S. R. Gwaltney, C.-P. Hsu, Y. Jung, J. Kong, D. S. Lambrecht, W. Liang, C. Ochsenfeld, V. A. Rassolov, L. V. Slipchenko, J. E. Subotnik, T. Van Voorhis, J. M. Herbert, A. I. Krylov, P. M. W. Gill and M. Head-Gordon, *Mol. Phys.*, 2015, **113**, 184–215.
- 16 R. S. Mulliken, *J. Am. Chem. Soc.*, 1952, **74**, 811–824.
- 17 N. S. Hush, Intervalence-Transfer Absorption. Part 2. Theoretical Considerations and Spectroscopic Data, in *Progress in Inorganic Chemistry*, ed. F. A. Cotton, John Wiley & Sons, Inc., Hoboken, NJ, USA, 2007, pp. 391–444.
- 18 N. S. Hush, *Electrochim. Acta*, 1968, **13**, 1005–1023.
- 19 J. R. Reimers and N. S. Hush, *J. Phys. Chem.*, 1991, **95**, 9773–9781.
- 20 C. Creutz, M. D. Newton and N. Sutin, *J. Photochem. Photobiol. A Chem.*, 1994, **82**, 47–59.

- 21 M. Rust, J. Lappe and R. J. Cave, *J. Phys. Chem. A*, 2002, **106**, 3930–3940.
- 22 S.-J. Lee, H.-C. Chen, Z.-Q. You, K.-L. Liu, T. J. Chow, I.-C. Chen and C.-P. Hsu, *Mol. Phys.*, 2010, **108**, 2775–2789.
- 23 J. E. Subotnik, S. Yeganeh, R. J. Cave and M. A. Ratner, *J. Chem. Phys.*, 2008, **129**, 244101.
- 24 C.-P. Hsu, *Acc. Chem. Res.*, 2009, **42**, 509–518.
- 25 J. L. Brédas, D. Beljonne, V. Coropceanu and J. Cornil, *Chem. Rev.*, 2004, **104**, 4971–5003.
- 26 V. Lemaire, M. Steel, D. Beljonne, J.-L. Brédas and J. Cornil, *J. Am. Chem. Soc.*, 2005, **127**, 6077–6086.
- 27 L. Cupellini, P. Wityk, B. Mennucci and J. Rak, *Phys. Chem. Chem. Phys.*, 2019, **21**, 4387–4393.
- 28 R. A. Marcus, *J. Chem. Phys.*, 1965, **43**, 679–701.
- 29 P. Song, Y. Li, F. Ma, T. Pullerits and M. Sun, *Chem. Rec.*, 2016, **16**, 734–753.
- 30 T. Liu and A. Troisi, *J. Phys. Chem. C*, 2011, **115**, 2406–2415.
- 31 L. Pandey, PhD Thesis, Georgia Institute of Technology, 2013.
- 32 U. C. Singh and P. A. Kollman, *J. Comput. Chem.*, 1984, **5**, 129–145.
- 33 B. H. Besler, K. M. Merz and P. A. Kollman, *J. Comput. Chem.*, 1990, **11**, 431–439.
- 34 S. Hirata and M. Head-Gordon, *Chem. Phys. Lett.*, 1999, **314**, 291–299.
- 35 A. D. Becke, *J. Chem. Phys.*, 1993, **98**, 5648–5652.
- 36 C. Lee, W. Yang and R. G. Parr, *Phys. Rev. B*, 1988, **37**, 785–789.
- 37 T. Yanai, D. P. Tew and N. C. Handy, *Chem. Phys. Lett.*, 2004, **393**, 51–57.